

RESEARCH ARTICLE

Open Access



# Intraoperative capsule protection can reduce the potential risk of adjacent segment degeneration acceleration biomechanically: an in silico study

Fei Huang<sup>1</sup>, Gang Huang<sup>4</sup>, Junpengli Jia<sup>4</sup>, Shihao Lu<sup>3\*</sup> and Jingchi Li<sup>2,4\*</sup>

## Abstract

**Background** The capsule of the zygapophyseal joint plays an important role in motion segmental stability maintenance. Iatrogenic capsule injury is a common phenomenon in posterior approach lumbar interbody fusion operations, but whether this procedure will cause a higher risk of adjacent segment degeneration acceleration biomechanically has yet to be identified.

**Methods** Posterior lumbar interbody fusion (PLIF) with different grades of iatrogenic capsule injury was simulated in our calibrated and validated numerical model. By adjusting the cross-sectional area of the capsule, different grades of capsule injury were simulated. The stress distribution on the cranial motion segment was computed under different loading conditions to judge the potential risk of adjacent segment degeneration acceleration.

**Results** Compared to the PLIF model with an intact capsule, a stepwise increase in the stress value on the cranial motion segment can be observed with a step decrease in capsule cross-sectional areas. Moreover, compared to the difference between models with intact and slightly injured capsules, the difference in stress values was more evident between models with slight and severe iatrogenic capsule injury.

**Conclusion** Intraoperative capsule protection can reduce the potential risk of adjacent segment degeneration acceleration biomechanically, and iatrogenic capsule damage on the cranial motion segment should be reduced to optimize patients' long-term prognosis.

**Keywords** Zygapophyseal joint, Capsule, Motion segment, Biomechanical deterioration, Iatrogenic capsule injury, Posterior lumbar interbody fusion

\*Correspondence:

Shihao Lu  
luwangda0309@163.com  
Jingchi Li  
Lijingchi9405@163.com

Full list of author information is available at the end of the article



© The Author(s) 2024. **Open Access** This article is licensed under a Creative Commons Attribution 4.0 International License, which permits use, sharing, adaptation, distribution and reproduction in any medium or format, as long as you give appropriate credit to the original author(s) and the source, provide a link to the Creative Commons licence, and indicate if changes were made. The images or other third party material in this article are included in the article's Creative Commons licence, unless indicated otherwise in a credit line to the material. If material is not included in the article's Creative Commons licence and your intended use is not permitted by statutory regulation or exceeds the permitted use, you will need to obtain permission directly from the copyright holder. To view a copy of this licence, visit <http://creativecommons.org/licenses/by/4.0/>. The Creative Commons Public Domain Dedication waiver (<http://creativecommons.org/publicdomain/zero/1.0/>) applies to the data made available in this article, unless otherwise stated in a credit line to the data.

## Introduction

Lumbar degenerative disease (LDD) is a common disease in elderly patients [1, 2]. With the increasing aging tendency in our country, the population base of the disease is step expanding [3, 4]. Degenerative changes in intervertebral disks (IVD) and zygapophyseal joints (ZJ) are the main pathological changes in LDD patients, and biomechanical deterioration initially triggers degeneration of these structures [5, 6]. Posterior approach lumbar interbody fusion (PLIF) is an effective method for the treatment of LDD [7, 8]. Adjacent segment disease (ASD) is a common postoperative complication. Related clinical symptom recurrence and revision surgery are the main triggers for poor long-term prognosis and social-economic burden [9, 10]. As a special kind of LDD, biomechanical deterioration caused by improper intraoperative procedures is also the initial trigger for ASD [9, 11]. In contrast, the optimization of surgical strategies may effectively reduce the risk of ASD by alleviating biomechanical deterioration [12, 13].

The lumbar spine is a complex structure consisting of various active and passive motion structures. The capsule of ZJ is an important structure for restricting the motion ranges in a special motion segment [14, 15]. Therefore, damage to the capsule may trigger segmental instability and resulting degeneration acceleration [16, 17]. To fully expose the pedicle screw insertion point, some surgeons completely destroy the dorsal side of the capsule [18, 19]. Based on above foundations, we hypothesize that iatrogenic capsule injury may trigger a higher risk of ASD, but this topic has yet to be identified in published studies. To verify this hypothesis, the biomechanical significance of capsule protection in the PLIF operation was validated by numerical mechanical simulations. To ensure the credibility of computed results, the model used in surgical simulations was calibrated and validated by comparing computed stress and motility characteristics values and mechanical tested values in published studies. To our knowledge, this was the first study to identify this topic.

## Material and methods

### Construction of the intact model

Simulations of PLIF with different grades of iatrogenic capsule injury have been performed in our previously constructed, calibrated, and validated numerical model. The detailed model construction, calibration, and validation strategy have been well described in these studies [20, 21]. Overall, the main purpose of these procedures was to improve the computational reliability, which is reflected in various aspects [22, 23]. First, the irregular surface of the reconstructed model was completely replaced by regular surfaces in the current spinal model.

By using this method, the incidence of computational error is significantly reduced [20, 21]. When constructing bony structure models, the thickness of cortical shell was defined as 0.8 mm, and the only exception was bony endplates (BEPs). Concave angles and depth of BEPs have been defined according to imaging and anatomical studies [24–26]. Moreover, when it comes to the construction of non-bony component numerical models, IVD consisted of annulus, nucleus, and cartilage endplates (CEP). The outline of the BEP covers entire cranial and caudal surfaces of IVD, while that of the CEP covers the nucleus and the inner half part of the annulus (Fig. 1) [27–29].

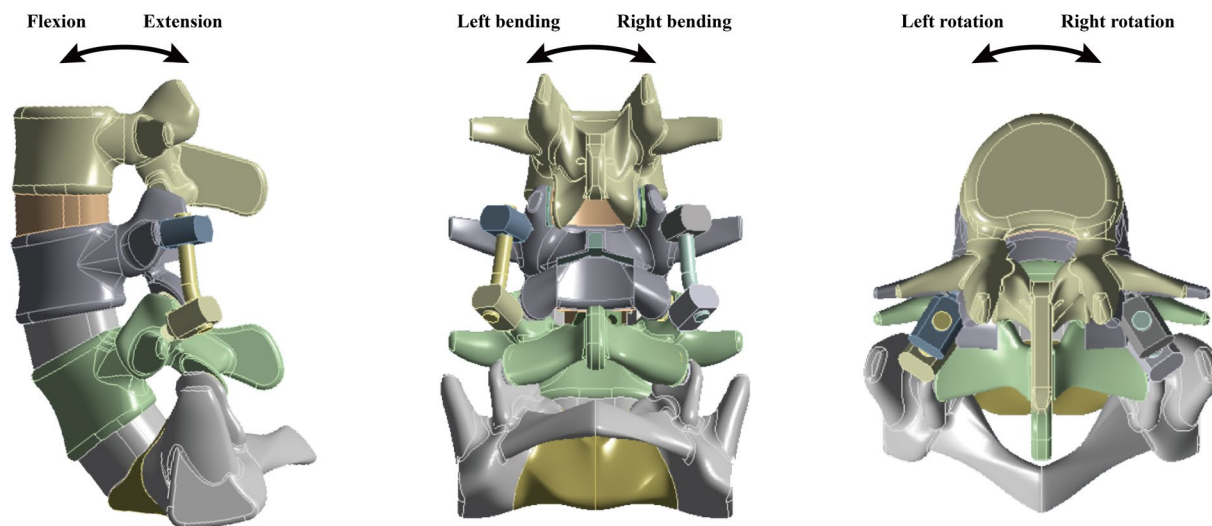
### Material property definition and model calibration

Mechanical material properties of different components were defined separately [30–32]. The cortical and cancellous bones were defined using the anisotropic law, while the remaining components were considered isotropic materials. Given that the stiffness of the ligaments was highly adjustable, a significant individual difference in this parameter existed, which was selected as the model calibration parameter. By adjusting the stiffness of ligaments under different loading conditions, the computed range of motion (ROM) is prone to the average ROM value from mechanical tests [33, 34]. Moreover, given that ligamentum structures suffer large deformations, the construction of solid element ligamentum models may trigger a high incidence of computational error. Therefore, line bodies were selected to construct ligament models, including all ligaments and the capsule of the articular process.

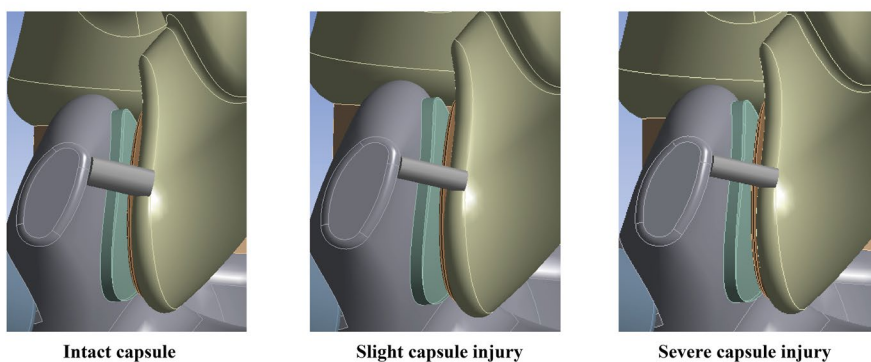
### Multi-indicators model validation

Given that the motility characteristics were a main perspective of the biomechanical environment, this calibration strategy could optimize the computational stability. In addition, multi-indicator model validation was also performed in this model. Consistent with the model calibration process, computational results from the calibrated model were also compared to the mechanical test results. The ROM, disk compression (DC) value, facet contact force (FCF), and intradiscal pressure (IDP) were compared between the computed and tested models [35–37]. When the difference between the computed and tested values was less than one standard deviation of the mechanical test, we believe that the current model was well validated. Finally, studies show that the size of elements will affect the computational result. To eliminate this confounding effect, mesh convergence tests were also performed in the validated model. The IDP value was selected as the reference of this test. When

**Simulation of PLIF in the L4-L5 motion segment and corresponding loading conditions.**



**Models with different capsules' cross-sectional areas**



**Screw trajectory definition**

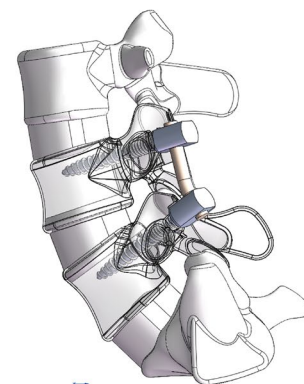


**Fig. 1** Schematic for PLIF simulations, loading conditions, different grades of capsule damage, and screw trajectories

the difference in IDP was smaller than 3% under different mesh sizes, we judged that the mesh convergence test was accomplished [22, 23]. In summary, in

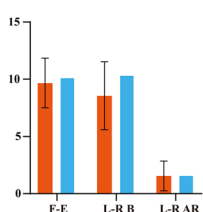
our published studies, we perform above-mentioned procedures to optimize the computational reliability of current numerical models (Fig. 2).

**Multi-indicators model validation**

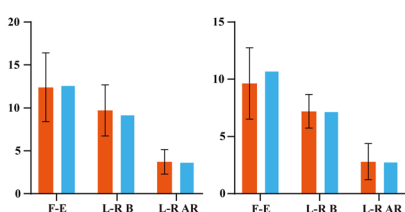
**Range of motion (°)**

F: 8Nm, E: 6Nm, B: 6Nm, AR: 4Nm

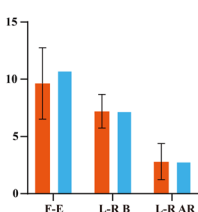
L3-L4 FSU



L4-L5 FSU

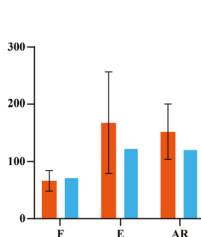


L5-S1 FSU



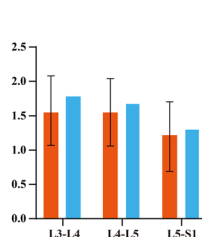
**Intradiscal pressure (KPa)**

7.5 Nm



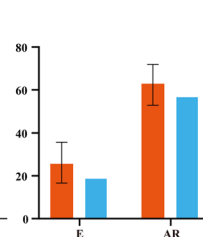
**Disc compression (mm)**

7.5 Nm



**Facet contact force (N)**

7.5 Nm



■ Mechanical tested results ■ Computed results

**Fig. 2** Multi-indicators model validation (consisted to our published studies)

### PLIF simulations with different grades of capsule iatrogenic injury

The simulation of the PLIF operation was performed by referring to the same type of studies and our clinical experience. Specifically, consistent with our published studies, the L4–L5 motion segment was selected in the PLIF simulation for the highest incidence of lumbar degenerative disease in this segment [6, 38, 39]. When simulating nerve structure decompression, the spinous process, the lower two-thirds of the laminae, the medial third of the inferior articular process of the L4 vertebral body, and the supraspinous and interspinous ligaments were excised [40, 41]. The posterior part of the annulus and all nuclei in the L4–L5 motion segment were excised to simulate discectomy, and the cartilage endplate of both the cranial and caudal sides of L4–L5 was also excised to simulate the endplate preparation process [8, 41].

To simulate the pedicle screw fixed interbody fusion operation, bilateral pedicle screws were inserted into the L4 and L5 vertebral bodies. When constructing pedicle screw models, the screw tulip and nut were simplified to a simple structure [42, 43]. By using this method, the contact between these two structures can be simplified to achieve simplification of the model and reduce the computational burden. Consistent with our published studies, the screw trajectory was parallel to the superior bony endplate in the corresponding vertebral body on the sagittal plane and parallel to the axis of the pedicle on the transverse plane [42, 43]. In addition, the elastic modulus of bony structures around the screw trajectory was adjusted. The range of adjusted bony structures consisted of the volume of screw. To eliminate the confounding effect caused by thread preservation, all threads were completely inserted into bony structures. When simulating cage insertion, a 26-mm cage filled with bone tissue was inserted into the interbody space from the right side of the interbody space. The material properties of bone tissue were defined according to our published studies [22, 30, 44]. Finally, as mentioned above, line bodies were selected to construct capsule models. Therefore, the cross-sectional area of the capsule was reduced to simulate different grades of intraoperative iatrogenic capsule injury. One-fourth and one-half cross-sectional area reduction of the L3–L4 capsule (the motion segment cranial to the surgical segment) were performed to construct PLIF models with slight and severe capsule injury (Fig. 1).

### Boundary and loading conditions

The boundary and loading conditions of ASD value computation consisted of the computation of ROM in the model calibration process. By selecting this model computation strategy, the computational reliability can be

effectively ensured. Specifically, the inferior surfaces of the PLIF models were completely fixed under all degrees of freedom, and different directional moments, including 8-Nm flexion, 6-Nm extension, left and right bending, and 4-Nm left and right directional axial rotation, were applied on the superior surface of L3 (Fig. 1) [22, 23]. The craniofacial coefficient between bone–screw interfaces and cage–bone interfaces was 0.2, and that between grafted bone and bony endplates was 0.46 [22, 23].

### Results

To evaluate the potential risk of cranial motion segmental ASD, IDP, FCF, and the maximum stress on the annulus were computed and recorded in this study. It is worth noting that under bending and rotation loading conditions, only facet contact on the contralateral side can be recorded. In other words, only the right-side FCF can be recorded and vice versa. A similar variation tendency of the computational result can be observed under almost all loading conditions. Specifically, a higher stress value can be observed with a reduction in the capsule cross-sectional area. In this process, a slight biomechanical deterioration can be recorded in the model with slight capsule injury, and obvious stress concentration can also be recorded in the model with one-half capsule cross-sectional area reduction. More significantly, compared to the difference between models with slight intact capsule and capsule injury, the difference between models with slight and severe capsule injury is more obvious. The most obvious biomechanical change can be observed under the extension loading condition. Compared to the model with an intact capsule, the IDP value in the model with severe capsule injury increased by more than 50%, the maximum annulus equivalent stress increased by 40%, and the value of FCF even increased by 60% (Figs. 3 and 4, Tables 1, 2, and 3).

### Discussion

Posterior approach lumbar interbody fusion is a common surgical strategy to treat LDD patients [19, 45]. The incidence of facet joint injury and the damage of ZJ capsule were nearly one-half in the pedicle insertion process [46, 47]. In which, intraoperative iatrogenic capsule injury is common to expose the bone structure around entry point of the pedicle screw. Considering that the capsule is an important structure of segmental stability maintenance, and segmental instability is a main reason for segmental degeneration acceleration, this procedure may trigger a higher risk of ASD in the cranial motion segment biomechanically after the lumbar interbody fusion operation. To verify this hypothesis, PLIF models with different grades of capsule injury were constructed based on a well-validated model constructed in our published

Computational results and corresponding variation tendency

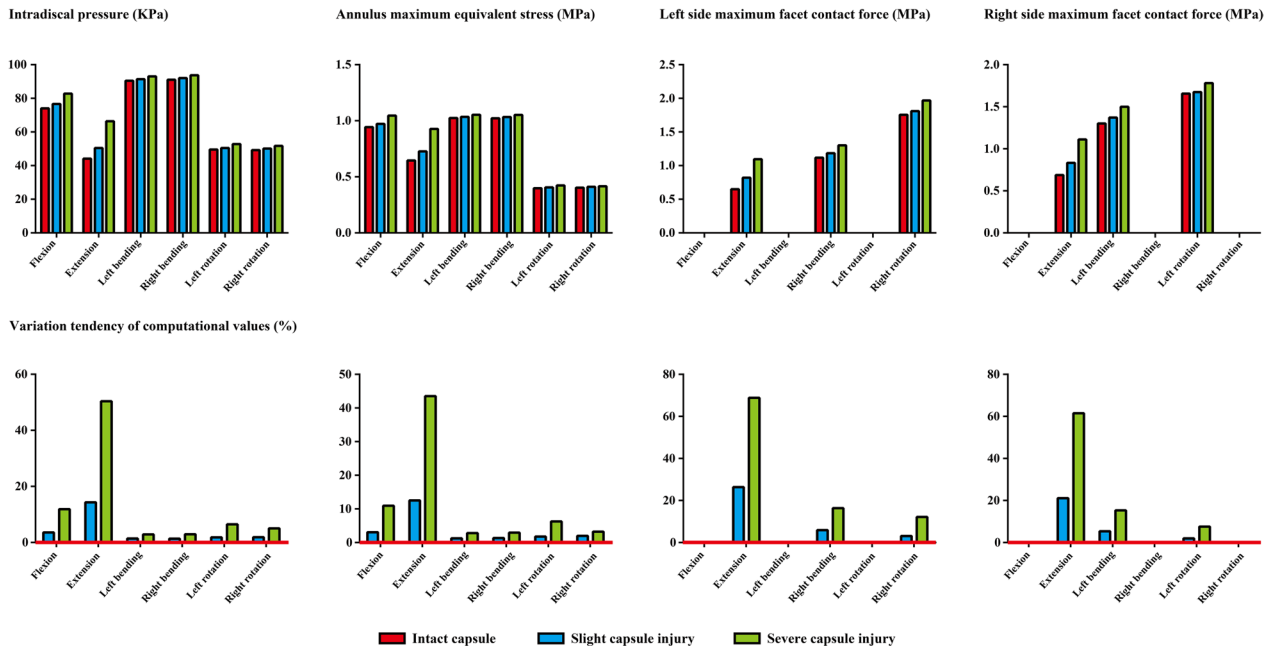
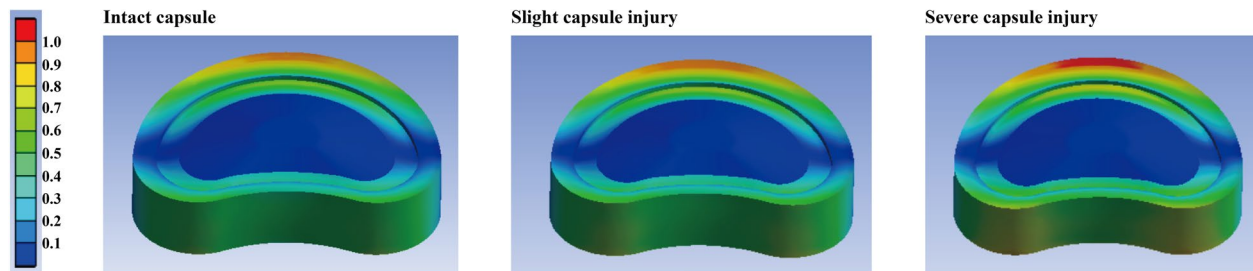


**Fig. 3** Computational results and variation tendency caused by capsule damage

Flexion



Extension

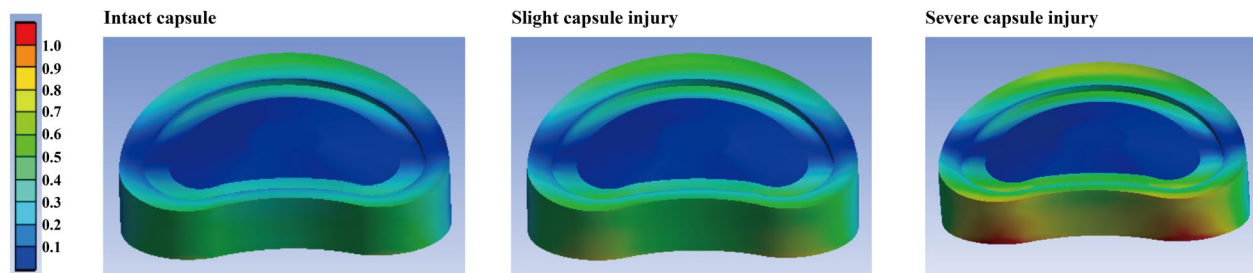


**Fig. 4** Nephograms of annulus distribution under flexion and extension loading conditions

studies, and stress values related to ASD were computed and recorded in this study.

The results show that capsule injury will lead to the deterioration of the stress value of the corresponding motion segment and trigger a higher risk of ASD

biomechanically. More importantly, only a slight biomechanical deterioration can be observed in the model with slight capsule injury (Figs. 3 and 4, Tables 1, 2, and 3). Based on the current computational results, although it may be impractical to completely avoid intraoperative

**Table 1** Computed intradiscal pressure in different models (KPa)

	Intact capsule	Slight capsule injury	Severe capsule injury
Flexion	74	76.66	82.77
Extension	44.15	50.47	66.39
Left bending	90.45	91.37	93.05
Right bending	91.05	92.01	93.71
Left rotation	49.55	50.45	52.76
Right rotation	49.2	50.12	51.67

**Table 2** Computed annulus maximum stress in different models (MPa)

	Intact capsule	Slight capsule injury	Severe capsule injury
Flexion	0.943	0.972	1.046
Extension	0.646	0.727	0.927
Left bending	1.024	1.034	1.053
Right bending	1.022	1.033	1.052
Left rotation	0.398	0.405	0.423
Right rotation	0.403	0.411	0.416

**Table 3** Computed left FCF in different models (MPa)

	Intact capsule	Slight capsule injury	Severe capsule injury
<i>Flexion</i>			
Extension	0.648	0.819	1.094
<i>Left bending</i>			
Right bending	1.118	1.184	1.301
<i>Left rotation</i>			
Right rotation	1.755	1.809	1.968

capsule injury (capsules may obscure the entry point of the pedicle, especially in patients with articular process hypertrophy), reducing the extent of capsule injury is still recommended to alleviate cranial segmental biomechanical deterioration and corresponding risk of ASD. Moreover, given that the most dramatic stress concentration can be recorded under the extension loading condition, this study also proves that the biomechanical significance of the capsule, and even of ZJ, is most significant under this loading condition. This conclusion was consistent with the same type of studies [48, 49].

The following aspects should be clarified from the methodological perspective. First, only stress values on the cranial motion segment were recorded in this study.

**Table 4** Computed right FCF in different models (MPa)

	Intact capsule	Slight capsule injury	Severe capsule injury
<i>Flexion</i>			
Extension	0.688	0.833	1.111
Left bending	1.301	1.371	1.5
<i>Right bending</i>			
Left rotation	1.656	1.674	1.781
Right rotation			

This is because the incidence of cranial ASD was significantly higher than that of caudal ASD [9, 50]: Surgical segmental high stiffness is the main reason for ASD biomechanically. Compared to the caudal side, given that the pedicle screw was more prone to the cranial position, more obvious stress concentration can be observed on the cranial side after the PLIF operation [12, 50, 51]. More significantly, from the clinical perspective, intraoperative injury of the caudal side capsule is not necessary. Therefore, these factors should not be investigated in this study (Table 4).

IDP, annulus maximum stress, and FCF were computed and recorded to represent potential risk of ASD. Stress concentration on the annulus and higher IDP values was proved to be risk factors for annulus tears [52, 53]. In the lumbar spine, annulus tear is the main phonological phenotype for IVD degeneration and LDD progression [6, 15]. Considering higher annulus stress and IDP values can be observed in models with iatrogenic capsule injury, we can deduce that this procedure may trigger higher risk of IVD degeneration and resulting ASD. In addition, FCF has also been computed to judge ASD risk. This is because the pathological process of ASD is not limited to degeneration of the intervertebral disk, acceleration degeneration of ZJ, and corresponding spinal canal stenosis, which is also an important pathological type of ASD [54, 55], especially for elderly patients (an epidemiological study reported that spinal canal stenosis, rather than lumbar disk herniation, is the main reason for lumbar surgery in elderly patients) [41, 55, 56]. In a word, by comprehensively computing IDP, annulus stress, and FCF, the current numerical models can good represent potential risk of ASD biomechanically.

Besides, pure moments, rather than moments with compressive load, were applied on current models for following reasons. Firstly, there are large individual differences in the amount of compressive load, and which was significantly influenced by weight of patients [32, 44]. In contrast, moment is a relatively

constant indicator of lumbar motion [31, 39]. More significantly, calibration and validation process of the current numerical model was accomplished under pure moments [20, 21]. The computational credibility of the current study can be ensured by computing mechanical parameters under the loading condition with model calibration and validation.

Meanwhile, endplate damage was also an important reason for intervertebral disk degeneration, but stress distribution on the endplate was not recorded in his study. Acute trauma is the main reason for endplate damage and the resulting acceleration of IVD degeneration. However, the loading conditions selected in this study were to simulate those in patients' daily lives [6, 15]. Therefore, endplate damage will not occur in this injury type. Finally, only one-half cross-sectional area reduction was selected when simulating severe capsule injury. When performing posterior approach lumbar surgery, the capsule on the ventral side cannot be injured; therefore, in the severe capsule injury model, one-half of the capsule cross-sectional area was reduced to simulate complete injury of the dorsal side capsule. In summary, the basic mechanism of ASD and the real situation of intraoperative situations were the main references for the currently selected model construction strategy.

Admittedly, the following limitations still existed in this study. First, capsule suffered large deformation under current loading conditions, solid element with large deformation values suffers high incidence of computational error [22, 31]. Therefore, line bodies, rather than solid elements, were selected for capsule model construction to ensure analysis convergence [33, 57]. Limited by this model construction strategy, the biomechanical significance of the capsule in different special regions cannot be identified in current models. We will try to perform numerical simulations by using different analysis modules, such as the dynamics computational module, to further verify the current computational results. In addition, our previous surgical records did not record the grade of capsule injury in detail and were limited by the ethical principle of clinical practice. Thus, the current biomechanical research conclusion cannot be validated by prospective clinical studies. The lack of clinical evidence is an important limitation of this study. Although these limitations existed, given that a consistent and obvious variation tendency can be observed in current models under different loading conditions, we still believe that the current research conclusion is reliable and should be revalidated in our future studies with further optimized models.

#### Author contributions

Fei Huang and Jingchi Li helped in conception and design; Fei Huang and Jingchi Li helped in model construction and finite element analysis; Gang Huang, Junpengli Jia, and Shihao Lu helped in analysis and interpretation of data; Fei Huang and Gang Huang helped in figures preparation; Fei Huang and Jingchi Li helped in manuscript preparation; and Shihao Lu and Jingchi Li helped in manuscript modification.

#### Funding

Not applicable.

#### Availability of data and materials

All the data of the manuscript are presented in the paper.

#### Declarations

#### Ethics approval and consent to participate

Not applicable.

#### Consent for publication

Not applicable.

#### Competing interests

The authors declare that they have no competing interests.

#### Author details

<sup>1</sup>Department of Orthopedics, Meishan Hospital of Traditional Chinese Medicine, Meishan, China. <sup>2</sup>Department of Orthopedics, The Affiliated Traditional Chinese Medicine Hospital, Southwest Medical University, No. 182, Chunhui Road, Longmatan District, Luzhou 646000, Sichuan Province, People's Republic of China. <sup>3</sup>Department of Orthopedics, Changzheng Hospital Affiliated to the Naval Medical University, Xiangyin Road, Shanghai 200433, People's Republic of China. <sup>4</sup>Luzhou Key Laboratory of Orthopedic Disorders, Southwest Medical University, No. 182, Chunhui Road, Luzhou 646000, Sichuan Province, People's Republic of China.

Received: 2 November 2023 Accepted: 9 January 2024

Published online: 16 February 2024

#### References

- Fehlings MG, Tetreault L, Nater A, Choma T, Harrop J, Mroz T, Santaguida C, Smith JS. The aging of the global population: the changing epidemiology of disease and spinal disorders. *Neurosurgery*. 2015;77(Suppl 4):S1-5.
- Heuck A, Glaser C. Basic aspects in MR imaging of degenerative lumbar disk disease. *Seminars Musculoskeletal Radiol*. 2014;18:228-39.
- Ferguson SJ, Steffen T. Biomechanics of the aging spine. *Eur Spine J*. 2003;12(Suppl 2):S97-s103.
- Lerner A, Mogensen MA, Kim PE, Shiroishi MS, Hwang DH, Law M. Clinical applications of diffusion tensor imaging. *World Neurosurg*. 2014;82:96-109.
- Adams MA, Dolan P. Biomechanics of vertebral compression fractures and clinical application. *Arch Orthop Trauma Surg*. 2011;131:1703-10.
- Adams MA, Dolan P. Intervertebral disc degeneration: evidence for two distinct phenotypes. *J Anat*. 2012;221:497-506.
- Athanasakopoulos M, Mavrogenis AF, Triantafyllopoulos G, Koufos S, Pneumatics SG. Posterior spinal fusion using pedicle screws. *Orthopedics*. 2013;36:e951-957.
- Goh JC, Wong HK, Thambyah A, Yu CS. Influence of PLIF cage size on lumbar spine stability. *Spine (Phila Pa 1976)* 2000; 25:35-39; discussion 40.
- Bagheri SR, Alimohammadi E, Zamani Froushani A, Abdi A. Adjacent segment disease after posterior lumbar instrumentation surgery for degenerative disease: incidence and risk factors. *J Orthop Surg (Hong Kong)*. 2019;27:2309499019842378.
- Bydon M, Macki M, Kerezoudis P, Sciubba DM, Wolinsky JP, Witham TF, Gokaslan ZL, Bydon A. The incidence of adjacent segment disease after lumbar discectomy: a study of 751 patients. *J Clin Neurosci*. 2017;35:42-6.

11. Ou CY, Lee TC, Lee TH, Huang YH. Impact of body mass index on adjacent segment disease after lumbar fusion for degenerative spine disease. *Neurosurgery* 2015; 76:396–401; discussion 401–392; quiz 402.
12. Hashimoto K, Aizawa T, Kanno H, Itoi E. Adjacent segment degeneration after fusion spinal surgery—a systematic review. *Int Orthop*. 2019;43:987–93.
13. Lee JC, Kim Y, Soh JW, Shin BJ. Risk factors of adjacent segment disease requiring surgery after lumbar spinal fusion: comparison of posterior lumbar interbody fusion and posterolateral fusion. *Spine (Phila Pa 1976)* 2014; 39:E339–345.
14. Adams MA, Freeman BJ, Morrison HP, Nelson IW, Dolan P. Mechanical initiation of intervertebral disc degeneration. *Spine (Phila Pa 1976)* 2000;25:1625–36.
15. Adams MA, Roughley PJ. What is intervertebral disc degeneration, and what causes it? *Spine (Phila Pa 1976)* 2006;31:2151–61.
16. Hsieh YY, Chen CH, Tsuang FY, Wu LC, Lin SC, Chiang CJ. Removal of fixation construct could mitigate adjacent segment stress after lumbosacral fusion: a finite element analysis. *Clin Biomech (Bristol, Avon)*. 2017;43:115–20.
17. Kaito T, Hosono N, Mukai Y, Makino T, Fujii T, Yonenobu K. Induction of early degeneration of the adjacent segment after posterior lumbar interbody fusion by excessive distraction of lumbar disc space. *J Neurosurg Spine*. 2010;12:671–9.
18. Oh KW, Lee JH, Lee JH, Lee DY, Shim HJ. The correlation between cage subsidence, bone mineral density, and clinical results in posterior lumbar interbody fusion. *Clin Spine Surg*. 2017;30:E683–e689.
19. Schnake KJ, Rappert D, Storzer B, Schreyer S, Hilber F, Mehren C. Lumbar fusion-Indications and techniques. *Der Orthopade*. 2019;48:50–8.
20. Li J, Xu C, Zhang X, Xi Z, Sun S, Zhang K, Fang X, Xie L, Liu Y, Song Y. Disc measurement and nucleus calibration in a smoothed lumbar model increases the accuracy and efficiency of in-silico study. *J Orthop Surg Res*. 2021;16:498.
21. Xu C, Xi Z, Fang Z, Zhang X, Wang N, Li J, Liu Y. Annulus calibration increases the computational accuracy of the lumbar finite element model. *Global Spine J*. 2022;21925682221081224.
22. Li JC, Xie TH, Zhang Z, Song ZT, Song YM, Zeng JC. The mismatch between bony endplates and grafted bone increases screw loosening risk for OLIF patients with ALSR fixation biomechanically. *Front Bioeng Biotechnol*. 2022;10:862951.
23. Li JC, Yang ZQ, Xie TH, Song ZT, Song YM, Zeng JC. Deterioration of the fixation segment's stress distribution and the strength reduction of screw holding position together cause screw loosening in ALSR fixed OLIF patients with poor BMD. *Front Bioeng Biotechnol*. 2022;10:922848.
24. Zhao FD, Pollintine P, Hole BD, Adams MA, Dolan P. Vertebral fractures usually affect the cranial endplate because it is thinner and supported by less-dense trabecular bone. *Bone*. 2009;44:372–9.
25. Liu JT, Han H, Gao ZC, He CY, Cai X, Niu BB, Gu MC, Li YH, Liang H, He XJ. CT assisted morphological study of lumbar endplate. *Zhongguo gu shang = China J Orthopaedics Traumatol*. 2018; 31:1129–35.
26. Pan CL, Zhang BY, Zhu YH, Ma YH, Li MF, Wang X, Yang F, Li YQ, Zhu YH. Morphologic analysis of Chinese lumbar endplate by three-dimensional computed tomography reconstructions for helping design lumbar disc prosthesis. *Medicine*. 2021;100:e24583.
27. DeLucca JF, Cortes DH, Jacobs NT, Vresilovic EJ, Duncan RL, Elliott DM. Human cartilage endplate permeability varies with degeneration and intervertebral disc site. *J Biomech*. 2016;49:550–7.
28. Jacobs NT, Cortes DH, Pelloquin JM, Vresilovic EJ, Elliott DM. Validation and application of an intervertebral disc finite element model utilizing independently constructed tissue-level constitutive formulations that are nonlinear, anisotropic, and time-dependent. *J Biomech*. 2014;47:2540–6.
29. Jacobs E, Roth AK, Arts JJ, van Rhijn LW, Willems PC. Reduction of intradiscal pressure by the use of polycarbonate-urethane rods as compared to titanium rods in posterior thoracolumbar spinal fixation. *J Mater Sci Mater Med*. 2017;28:148.
30. Li J, Xie Y, Sun S, Xue C, Xu W, Xu C, Xi Z. Regional differences in bone mineral density biomechanically induce a higher risk of adjacent vertebral fracture after percutaneous vertebroplasty: a case-comparative study. *Int J Surg (London, England)* 2023.
31. Spina NT, Moreno GS, Brodke DS, Finley SM, Ellis BJ. Biomechanical effects of laminectomies in the human lumbar spine: a finite element study. *Spine J*. 2021;21:150–9.
32. Zhang Q, Chon T, Zhang Y, Baker JS, Gu Y. Finite element analysis of the lumbar spine in adolescent idiopathic scoliosis subjected to different loads. *Comput Biol Med*. 2021;136:104745.
33. Schmidt H, Heuer F, Drumm J, Klezl Z, Claes L, Wilke HJ. Application of a calibration method provides more realistic results for a finite element model of a lumbar spinal segment. *Clin Biomech (Bristol, Avon)*. 2007;22:377–84.
34. Li J, Xu C, Zhang X, Xi Z, Liu M, Fang Z, Wang N, Xie L, Song Y. TELD with limited foraminoplasty has potential biomechanical advantages over TELD with large annuloplasty: an in-silico study. *BMC Musculoskelet Disord*. 2021;22:616.
35. Renner SM, Natarajan RN, Patwardhan AG, Havey RM, Voronov LI, Guo BY, Andersson GB, An HS. Novel model to analyze the effect of a large compressive follower pre-load on range of motions in a lumbar spine. *J Biomech*. 2007;40:1326–32.
36. Schilling C, Krüger S, Grupp TM, Duda GN, Blömer W, Rohlmann A. The effect of design parameters of dynamic pedicle screw systems on kinematics and load bearing: an in vitro study. *Eur Spine J*. 2011;20:297–307.
37. Wilson DC, Niosi CA, Zhu QA, Oxland TR, Wilson DR. Accuracy and repeatability of a new method for measuring facet loads in the lumbar spine. *J Biomech*. 2006;39:348–53.
38. Pfirrmann CW, Metzendorf A, Zanetti M, Hodler J, Boos N. Magnetic resonance classification of lumbar intervertebral disc degeneration. *Spine (Phila Pa 1976)* 2001;26:1873–8.
39. Sengul E, Ozmen R, Yaman ME, Demir T. Influence of posterior pedicle screw fixation at L4–L5 level on biomechanics of the lumbar spine with and without fusion: a finite element method. *Biomed Eng*. 2021;20:98.
40. Kaito T, Hosono N, Fujii T, Makino T, Yonenobu K. Disc space distraction is a potent risk factor for adjacent disc disease after PLIF. *Arch Orthop Trauma Surg*. 2011;131:1499–507.
41. Mobbs RJ, Phan K, Malham G, Seex K, Rao PJ. Lumbar interbody fusion: techniques, indications and comparison of interbody fusion options including PLIF, TLIF, MI-TLIF, OLIF/ATP, LLIF and ALIF. *J Spine Surg (Hong Kong)*. 2015;1:2–18.
42. Huang C, Liu Z, Wei Z, Fang Z, Xi Z, Cai P, Li J. Will the adjustment of interslotted pedicle screw positions affect the risk of adjacent segment diseases biomechanically? An in-silico study. *Front Surg*. 2022;9:1004642.
43. Xu C, Huang C, Cai P, Fang Z, Wei Z, Liu F, Li J, Liu Y. Biomechanical effects of pedicle screw positioning on the surgical segment in models after oblique lumbar interbody fusion: an in-silico study. *Int J Gen Med*. 2022;15:1047–56.
44. Xi Z, Xie Y, Chen S, Sun S, Zhang X, Yang J, Li J. The cranial vertebral body suffers a higher risk of adjacent vertebral fracture due to the poor biomechanical environment in patients with percutaneous vertebralplasty. *Spine J*. 2023.
45. Kashii M, Kitaguchi K, Makino T, Kaito T. Comparison in the same intervertebral space between titanium-coated and uncoated PEEK cages in lumbar interbody fusion surgery. *J Orthopaedic Sci*. 2020;25:565–70.
46. Zeng ZL, Jia L, Xu W, Yu Y, Hu X, Jia YW, Wang JJ, Cheng LM. Analysis of risk factors for adjacent superior vertebral pedicle-induced facet joint violation during the minimally invasive surgery transforaminal lumbar interbody fusion: a retrospective study. *Eur J Med Res*. 2015;20:80.
47. Oh HS, Seo HY. The relationship between adjacent segment pathology and facet joint violation by pedicle screw after posterior Lumbar instrumentation surgery. *J Clin Med*. 2021;10.
48. Bermel EA, Barocas VH, Ellingson AM. The role of the facet capsular ligament in providing spinal stability. *Comput Methods Biomech Biomed Engin*. 2018;21:712–21.
49. Dunlop RB, Adams MA, Hutton WC. Disc space narrowing and the lumbar facet joints. *J Bone Joint Surg Br*. 1984;66:706–10.
50. Park P, Garton HJ, Gala VC, Hoff JT, McGillicuddy JE. Adjacent segment disease after lumbar or lumbosacral fusion: review of the literature. *Spine (Phila Pa 1976)* 2004;29:1938–44.
51. Zhong ZM, Deviren V, Tay B, Burch S, Berven SH. Adjacent segment disease after instrumented fusion for adult lumbar spondylolisthesis: Incidence and risk factors. *Clin Neurol Neurosurg*. 2017;156:29–34.
52. Sharma A, Lancaster S, Bagade S, Hildebolt C. Early pattern of degenerative changes in individual components of intervertebral discs in stressed and nonstressed segments of lumbar spine: an in vivo magnetic resonance imaging study. *Spine (Phila Pa 1976)* 2014;39:1084–90.



53. Ozer AF, Oktenoglu T, Sasani M, Kaner T, Ercelen O, Canbulat N. Unusual cause of acute low-back pain: sudden annulus fibrosus rupture. *Orthop Rev (Pavia)*. 2012;4:e22.
54. Khalaf K, Nikkhoo M. Comparative biomechanical analysis of rigid vs. flexible fixation devices for the lumbar spine: A geometrically patient-specific poroelastic finite element study. *Comput Methods Programs Biomed*. 2021; 212:106481.
55. Yokoyama K, Yamada M, Tanaka H, Ito Y, Sugie A, Wanibuchi M, Kawanishi M. Factors of adjacent segment disease onset after microsurgical decompression for lumbar spinal canal stenosis. *World Neurosurg*. 2020;144:e110–8.
56. Ruetten S, Komp M. Endoscopic lumbar decompression. *Neurosurg Clin N Am*. 2020;31:25–32.
57. Schmidt H, Heuer F, Simon U, Kettler A, Rohlmann A, Claes L, Wilke HJ. Application of a new calibration method for a three-dimensional finite element model of a human lumbar annulus fibrosus. *Clin Biomech (Bristol, Avon)*. 2006;21:337–44.

### **Publisher's Note**

Springer Nature remains neutral with regard to jurisdictional claims in published maps and institutional affiliations.